Influence of C_4 vegetation on $^{13}CO_2$ discrimination and isoforcing in the upper Midwest, United States

T. J. Griffis,[1] J. M. Baker,[1,2] S. D. Sargent,[3] M. Erickson,[1] J. Corcoran,[1] M. Chen,[1] and K. Billmark[1]

Received 22 December 2009; revised 13 May 2010; accepted 9 June 2010; published 26 October 2010.

[1] Agricultural crops with a C_4 photosynthetic pathway rapidly expanded across North America as early as 800 A.D. Their distribution continues to expand globally as demands for food and biofuel production increase. These systems are highly productive, having a significant impact on carbon and water exchange between the land and atmosphere. Here, we investigate the relative impact of agricultural C_4 vegetation on the $^{13}CO_2$ photosynthetic discrimination and atmospheric isotopic forcing in the upper Midwest, United States. We address three questions: (1) What is the relative importance of C_3 and C_4 species to the CO_2 budget? (2) How do these different photosynthetic pathways influence the photosynthetic discrimination within this heterogeneous landscape? (3) To what extent does land use change (i.e., a change in C_4 crops) impact atmospheric isotopic forcing and the isotopic signature of the atmosphere? These questions are addressed using measurements obtained from the University of Minnesota tall tower (244 m) trace gas observatory (TGO) over the growing seasons of 2007 and 2008 and are supported with scaled-up values of discrimination and isotopic forcing based on ecosystem-scale eddy flux observations and high-resolution land use data. Our land use analyses indicate that local and regional C_4 production was higher by 10% in 2007 due to increased demand for biofuel. The 2007 growing season was also characterized by moderate drought as a consequence of low antecedent soil water content. Isotopic flux ratio measurements from TGO provide evidence that the increase in C_4 land use and drier soil conditions of 2007 had a significant impact on the growing season $^{13}CO_2$ photosynthetic discrimination, which ranged from 11.5 to 14.8 in 2007 and 12.4‰ to 17.4‰ in 2008. Isotopic partitioning indicated that C_4 species accounted for about 20 to 40% of the growing season gross photosynthetic CO_2 exchange. The isoforcing analysis revealed that C_3 discrimination dominated the atmospheric δ_a^{13} budget, especially during spring and fall. Estimates of $^{13}CO_2$ photosynthetic discrimination for this region support recently published isotope modeling studies that explicitly accounted for increases in C_4 cropland, which has significant implications for estimating the terrestrial carbon sink strength based on inverse modeling techniques.

Citation: Griffis, T. J., J. M. Baker, S. D. Sargent, M. Erickson, J. Corcoran, M. Chen, and K. Billmark (2010), Influence of C_4 vegetation on $^{13}CO_2$ discrimination and isoforcing in the upper Midwest, United States, *Global Biogeochem. Cycles*, *24*, GB4006, doi:10.1029/2009GB003768.

1. Introduction

[2] The stable carbon isotope ratio, $^{13}CO_2/^{12}CO_2$, is a powerful tracer for examining questions related to impacts of land use changes on carbon cycling because it contains information about short-term (hours/days) and long-term (seasonal/interannual) dynamics. At hourly time scales, photosynthetic discrimination against the heavier $^{13}CO_2$ molecule causes photosynthetically fixed CO_2 to become relatively depleted in ^{13}C while the atmosphere becomes relatively enriched in ^{13}C [*Farquhar et al.*, 1989]. The amount of discrimination is strongly dependent on photosynthetic pathway (Calvin Cycle, C_3 versus Hatch-Slack Cycle, C_4) and is also influenced by other environmental factors such as precipitation, canopy conductance, vapor pressure deficit, and the ratio of stomatal to atmospheric CO_2 concentration [*Farquhar et al.*, 1989; *Yakir and Sternberg*, 2000; *Bowling et al.*, 2002; *Suits et al.*, 2005]. The isotopic composition of recently fixed photosynthate

[1]Department of Soil, Water, and Climate, University of Minnesota, Saint Paul, Minnesota, USA.
[2]USDA-ARS, St. Paul, Minnesota, USA.
[3]Campbell Scientific Incorporated, Logan, Utah, USA.

0886-6236/10/2009GB003768

(δ_P) is to some extent modulated by subsequent biochemical reactions during the formation of plant tissues, etc. [*Ghashghaie et al.*, 2001; *Tcherkez et al.*, 2003; *Badeck et al.*, 2005; *Bathellier et al.*, 2008]. This photosynthetic isotope signal is continuously recorded in the standing biomass and soil organic matter providing a tracer of environmental change over longer time scales.

[3] C_3 plants discriminate more strongly against $^{13}CO_2$ than C_4 plants. Carbon isotope composition of C_3 and C_4 leaves typically vary from about −28 to −26‰ and −15 to −13‰, respectively [*Farquhar*, 1983; *Farquhar et al.*, 1989; *Cerling et al.*, 1997]. These isotopic differences provide a unique opportunity to examine how C_3 and C_4 vegetation contribute to the local, regional, and global carbon budget. Variations in the relative abundance of C_3 and C_4 species can be linked to changes in climate, atmospheric CO_2 concentrations, and disturbance factors such as increased fire and fragmentation of forests [*Cerling et al.*, 1997; *Ehleringer et al.*, 1997; *Keeley and Rundel*, 2005; *Osborne and Beerling*, 2006; *Edwards and Still*, 2008]. Today, C_4 grasses are most dominant in warmer semiarid climates with moderate to high light levels [*Sage*, 2001]. In North America, the natural distribution of C_4 species in prairies has been significantly impacted by human disturbance and the development of an agricultural economy. The introduction of C_4 corn into Eastern North America likely occurred as early as A.D. 200 and rapidly expanded between A.D. 800 and 1100 as indicated from the carbon isotope ratio analysis of human bone collagen [*Smith*, 1989].

[4] Temporal and spatial variations in the relative C_3/C_4 contributions have significant implications for our understanding of the global carbon and water cycles [*Lloyd and Farquhar*, 1994; *Ehleringer et al.*, 1997; *Still et al.*, 2003a; *Suits et al.*, 2005]. C_4 species are estimated to account for about 17% to 23% of global gross primary productivity [*Wittenberg and Esser*, 1997; *Lloyd and Farquhar*, 1994; *Still et al.*, 2003a; *Ito*, 2003]. Determining the global distribution of the C_3 and C_4 photosynthetic pathways is essential for estimating the atmospheric budget of $^{13}CO_2$, $^{12}CO_2$ and $\delta^{13}C$-CO_2 (isoforcing) and constraining the regional carbon sink/source strength using the double deconvolution inverse method [*Lloyd and Farquhar*, 1994; *Still et al.*, 2003a; *Lai et al.*, 2004, 2006; *Scholze et al.*, 2008]. *Still et al.* [2003a] estimated the global coverage of C_4 and C_3 vegetation to be 18.8 million km^2 and 87.4 million km^2, respectively. Using SiB2, they modeled a gross primary production of 35.3 Pg C yr^{-1} and 114.7 Pg C yr^{-1}, for the C_4 and C_3 pathways and estimated photosynthetically weighted global terrestrial plant discrimination to be about 16.5‰. Using an isotopic mass balance approach they then estimated a net land uptake of 2.4 Pg C yr^{-1} and 1.4 Pg C yr^{-1} by the ocean. Such estimates are highly sensitive to the relative distribution of C_3/C_4 species and their influence on the photosynthetic discrimination. *Scholze et al.* [2008] recently noted that state-of-the-art inverse methods have ignored the effects of C_4 crops, which can cause the partitioning between oceanic and terrestrial carbon fluxes to change significantly. They demonstrated that ignoring the effects of C_4 crops caused the partitioning between oceanic and terrestrial carbon fluxes to shift by about 1 Pg C y^{-1}, with the terrestrial sink becoming smaller. Such a large change is significant and it exceeds the uncertainties in the inverse methodology [*Scholze et al.*, 2008].

[5] Globally, C_4 crops are grown on approximately 3.2 million km^2, representing 24% of all harvested land and 17% of C_4 vegetation [*Monfreda et al.*, 2008]. In the upper Midwest, United States, C_4 and C_3 rotation ecosystems (i.e., corn and soybean, respectively) dominate the landscape, covering about 150 million hectares. Changing demands for agriculture and biofuel can cause significant perturbations in land use and management. For example, in 2007 corn production was increased (relative to the average over the period 2000 to 2006) by ≈0.5 and 6 million hectares in Minnesota and the United States, respectively [*USDA-NASS*, 2007b] to satisfy rising ethanol demands [*Donner and Kucharik*, 2008]. Recent model simulations by *Donner and Kucharik* [2008] indicate that an increase in corn acreage of more than 60% will be required to meet the 36 billion gallon biofuel goal by the year 2022 as outlined by the United States Energy Policy Act. A perturbation in land use (*via* photosynthetic pathway or environmental conditions) can change the isotopic composition of photosynthesis (δ_P), ecosystem respiration (δ_R) or the land isotopic disequilibrium ($D_L = \delta_R - \delta_P$). These key parameters are used by the inverse modeling community to help constrain the partitioning of carbon sink/source strength of the ocean and land [*Ciais et al.*, 1995; *Fung et al.*, 1997; *Rayner et al.*, 1999; *Ito*, 2003; *Scholze et al.*, 2008; *Rayner et al.*, 2008]. Further, a perturbation in land use is expected to have a significant influence on the isotopic forcing of the atmosphere [*Lee et al.*, 2009].

[6] Detection and interpretation of such changes, however, requires that state-of-the-art models [*Fung et al.*, 1997; *Ito*, 2003; *Riley et al.*, 2002] be constrained by routine and direct measurement of the relevant isotopic fluxes at the appropriate temporal and spatial scales. At the present time we do not have a network of isotopic flux measurement sites, analogous to Global Fluxnet, that can provide detailed information on isotopic CO_2 exchange and key discrimination parameters. Traditionally, these types of isotope data have been collected weekly or during short intensive campaigns by collecting air samples in flasks and using isotope ratio mass spectrometry analysis [*Keeling*, 1958; *Flanagan and Ehleringer*, 1998; *Bakwin et al.*, 1998; *Buchmann and Ehleringer*, 1998; *Pataki et al.*, 2003; *Miller et al.*, 2003; *Lai et al.*, 2004, 2006]. Advances in laser technologies [*Bowling et al.*, 2003; *Griffis et al.*, 2004; *Lee et al.*, 2005; *Griffis et al.*, 2008] are providing new capacity for near-continuous measurement of isotopic mixing ratios and fluxes that should provide better constraints on isotopic fluxes, discrimination, and data sets for model development and verification [*McDowell et al.*, 2008].

[7] The objectives of this paper are to (1) Examine the influence of C_4 vegetation on biosphere-atmosphere CO_2 exchange and ^{13}C discrimination at the mesoscale (≈5 km) within the upper Midwest, United States; (2) Assess the relative importance of C_4 species to the mesoscale carbon budget; and (3) Evaluate the potential influence of land use change on $^{13}CO_2$ discrimination and isoforcing. These objectives are addressed through analysis of carbon iso-

tope concentration and flux measurements obtained during the 2007/2008 growing seasons from the University of Minnesota tall tower (244 m) Trace Gas Observatory (TGO) located within an agricultural landscape near St. Paul, Minnesota, United States.

2. Theory

2.1. Biosphere-Atmosphere Isotopic CO_2 Exchange

[8] Concentration and flux measurements from tall towers can provide greater spatial information regarding the influence of land use and land surface heterogeneity on regional carbon budgets and isotopic discrimination [*Bakwin et al.*, 1998; *Yi et al.*, 2000; *Berger et al.*, 2001; *Davis et al.*, 2003; *Haszpra et al.*, 2005; *Marquis and Tans*, 2008; *Barcza et al.*, 2009], but the methodology presents a number of challenges that can make the interpretation of tall tower data difficult. Here we provide a brief overview of the eddy covariance (EC) approach and isotopic mass balance for CO_2 in order to discuss the methodological issues that are of particular interest to tall tower applications in heterogeneous terrain and to give appropriate background for the flux-based (EC and flux-gradient) approach to determining isotopic composition and isoforcing.

[9] *Yi et al.* [2000] reexamined the conservation equation of a scalar (c^i) for the application of tall tower flux measurements where horizontal and vertical advection can be significant. They argued that in convective conditions the horizontal turbulent flux divergence is small compared to the vertical flux divergence and noted that when the flux footprint is large relative to the spatial scale of the heterogeneity (for instance, if eddy scale is large compared to the dimensions of typical field crops) the horizontal flux divergence can be ignored. Following Reynolds decomposition and averaging, and ignoring molecular diffusivity and horizontal flux divergence, the conservation equation for c^i can be written as,

$$\frac{\partial \overline{c^i}}{\partial t} + \overline{u}\frac{\partial \overline{c^i}}{\partial x} + \overline{w}\frac{\partial \overline{c^i}}{\partial z} + \frac{\partial \overline{w'c^{i'}}}{\partial z} = \overline{s}_{c^i} \tag{1}$$

where, t is time, x is direction aligned with the horizontal mean wind, z is the direction perpendicular to the typical streamlines, w is the vertical wind velocity, c^i is the CO_2 concentration and superscript i indicates the isotopologue of interest ($^{13}CO_2$ or $^{12}CO_2$), the primes indicate the differences between instantaneous and mean values and the overbar indicates an averaging operation (60 min integration period). $\overline{w'c^{i'}}$ is the covariance of w and c^i. The left-hand-side terms represent the change in scalar concentration per unit time, horizontal advection, vertical advection, and turbulent vertical flux, respectively, and $\overline{s}_{ci}$ represents the sink/source term.

[10] The net ecosystem exchange of isotopic CO_2 (F_N^i) can be obtained from integration of equation (1) over the specified control volume,

$$F_N^i = \int_0^{z_r} \frac{\partial \overline{c^i}}{\partial t} dz + \left(\overline{w'c^{i'}}\right)_{z_r} + \int_0^{z_r} \left\{ \overline{u}\frac{\partial \overline{c^i}}{\partial x} + \overline{w}\frac{\partial \overline{c^i}}{\partial z} \right\} dz \tag{2}$$

where the terms on the right-hand side represent the rate of change in storage between the ground and EC measurement height (F_S^i), eddy flux (F_E^i), and the combination of horizontal and vertical advection (F_A^i),

$$F_N^i = F_S^i + F_E^i + F_A^i \tag{3}$$

[11] A number of studies have shown that the advective terms can be important especially when turbulence is weakly developed at night; at towers located within complex terrain; and on tall towers where top down diffusion can cause flux divergence [*Lee*, 1998; *Yi et al.*, 2000; *Finnigan*, 1999; *Wyngaard and Brost*, 1984; *Huang et al.*, 2008]. However, it has also been assumed that the advection terms are negligible over the long term (i.e., when ensemble averaged over a few synoptic cycles or phenological windows) [*Davis et al.*, 2003]. The importance of advection at TGO and other methodological details are provided in the auxiliary material.[1]

2.2. Isotopic Flux Ratio and Isotopic Forcing

[12] The isotopic signature of the net flux can be obtained from the flux ratio of equation (3) [*Griffis et al.*, 2004],

$$R_N = \frac{F_N^{13}}{F_N^{12}} \tag{4}$$

where the molar ratio R_N is computed from the ratio of the heavy to light isotopic fluxes and can be expressed in delta notation,

$$\delta_N = 1000\left(\frac{R_N}{R_{VPDB}} - 1\right) \tag{5}$$

where R_{VPDB} is the standard molar ratio based on the Vienna Peedee Belemnite scale.

[13] The flux ratio can also be obtained from the flux-gradient approach [*He and Smith*, 1999; *Griffis et al.*, 2004, 2007; *Drewitt et al.*, 2009]. In the case of taller towers, gradient measurements are susceptible to counter-gradient transport from large scales of motion and can result in an underestimate of the flux. Further, the large height differences between inlets results in different source/sink footprint functions. While these are legitimate concerns, we demonstrate later that both the EC and flux-gradient techniques produce similar results and that the flux-gradient approach yields significantly lower uncertainty. We believe that the relatively good agreement resulted from the fact that the inlets are located well above the roughness sublayer and that the land surface heterogeneity is consistent (self similarity) across spatial scales ranging from about 5 to 100 km from the tower (see details below).

[14] Equation (3) can also be written as an isoflux ($F_N\delta_N$, the product of the flux and its isotopic composition) [*Bowling et al.*, 2001],

$$F_N\delta_N = \left(\delta_a^{13} - \Delta\right)F_P + \delta_R F_R \tag{6}$$

[1] Auxiliary materials are available with the HTML. doi:10.1029/2009GB003768.

where δ_a^{13} is the isotopic composition of the boundary layer air. Δ and δ_R are the flux-weighted photosynthetic discrimination and isotope composition of respiration, respectively. F_P and F_R represent photosynthetic and respiratory fluxes. Here, we measured the isotopic flux ratio directly at the tall tower and we used equation (6) with observations at the ecosystem scale to calculate δ_N.

[15] Finally, the influence of biosphere-atmosphere CO_2 exchange on the atmospheric δ_a^{13} budget can be evaluated from the isotopic forcing (I_F) perspective [*Tans*, 1980; *Yakir*, 2003],

$$I_F = \frac{F_N}{C_a}\left(\delta_N - \delta_a^{13}\right) \tag{7}$$

where, C_a is the molar concentration of CO_2. Starting from equation (1), *Lee et al.* [2009] demonstrated that the covariance term, $\overline{w'\delta'}$, is mathematically identical to equation (7). $\overline{w'\delta'}$ represents the correct flux boundary condition driving the temporal variations in atmospheric δ_a^{13} and can be measured directly using eddy covariance and laser spectroscopy [*Griffis et al.*, 2008; *Lee et al.*, 2009]. Field-scale measurements of isotopic CO_2 exchange over C_3 and C_4 systems [*Griffis et al.*, 2005, 2007; *Zhang et al.*, 2006], within close proximity to the tall tower, were used to provide estimates of the isoforcing for the individual C_3 and C_4 components,

$$I_F = \gamma_3\overline{w'\delta_3'} + \gamma_4\overline{w'\delta_4'} = \frac{\gamma_3 F_{N_3}}{C_a}\left(\delta_{N_3} - \delta_a^{13}\right) + \frac{\gamma_4 F_{N_4}}{C_a}\left(\delta_{N_4} - \delta_a^{13}\right) \tag{8}$$

where γ_3 and γ_4 represent weighting factors determined from a flux footprint climatology (described in the auxiliary material). Further, we make use of traditional micrometeorological estimates of F_P (i.e., $F_P = F_N - F_R$) and canopy conductance (g_c) of CO_2 using the Penman-Monteith equation to help constrain the C_3 (g_{c3}) and C_4 (g_{c4}) photosynthetic discrimination factors,

$$\Delta_3 = b_3 + \left(b_3 - \epsilon_k^{13}\right)\frac{F_{P_3}}{g_{c3}C_a} \tag{9}$$

$$\Delta_4 = \epsilon_k^{13} + b' + \frac{F_{P_4}b'}{g_{c4}C_a} \tag{10}$$

where ϵ_k^{13} is the kinetic fractionation and b' is the enzymatic fractionation associated with the C_4 photosynthetic pathway,

$$b' = b_4 + b_3\phi - \epsilon_k^{13} \tag{11}$$

where b_3, b_4, and ϕ, are the enzymatic fractionation of Rubisco (27‰) and PEP carboxylase (−5.7‰) and the bundle sheath leakage parameter, respectively. ϕ was estimated by *Zhang et al.* [2006] to be 0.3 at this study site in 2003.

[16] Using equations (6) through (11), we provide estimates of $^{13}CO_2$ isotopic composition and isotopic forcing and compare these estimates with the tall tower observations. Together, these estimates are used to constrain the impact of land use on the $^{13}CO_2$ budget of the atmosphere and photosynthetic discrimination.

3. Materials and Methods

3.1. Research Site and Land Use History

[17] The tall tower (Minnesota Public Radio communications tower, KCMP 89.3 FM) is located approximately 25 km to the south of Minneapolis/St. Paul (44°41′19″N, 93°4′22″W; 290 m ASL) at the University of Minnesota, Rosemount Research and Outreach Center (RROC) (Figure 1). The tower was instrumented with two eddy covariance systems and one tunable diode laser in April 2007. Here we focus our analysis on the growing seasons of 2007 and 2008 from approximately DOY 152 (1 June) to DOY 274 (1 October). Two field-scale micrometeorological stations are also located at RROC within about 3 km of TGO and have been part of the AmeriFlux network since 2004 [*Baker and Griffis*, 2005]. These sites are currently in corn and soybean production and are used in this analysis for comparative purposes and to provide independent estimates of isotopic composition and isoforcing.

[18] Presettlement vegetation history within the tall tower flux footprint is upland dry prairie, consisting of C_3 and C_4 plant species with dominant species consisting of big bluestem (*Andropogon gerardii* Vitman), and Indian grass (*Sorghastrum nutans*) [*Marschner*, 1974]. Significant production of wheat, oats, corn and potato within the region occurred as early as 1860 according to the Minnesota State Agricultural Census Data, Dakota County Historical Society.

3.2. Land Cover Data and Analyses

[19] Regional land cover data products included the 2007/2008 USDA-NASS Crop Data Layer (CDL).The CDL product has a 56 m spatial resolution and was validated using ground reference data for agricultural areas including traditional data from the Farm Service Agency (FSA) Common Land Unit (CLU) program [*USDA-NASS*, 2007a; *Homer et al.*, 2007]. In addition, a hybrid supervised/unsupervised land use classification scheme was developed using a combination of air photos, ground reference data near the tall tower, and Landsat TM images in 2007/2008 to develop 30 m resolution land use maps for flux footprint analyses [*Corcoran*, 2009]. The hybrid classification scheme was found to have a level 2 (i.e., corn, soybean, other crop land use) accuracy of 71% [*Corcoran*, 2009]. Flux footprint/land use analysis and estimation of the normalized difference vegetation index (NDVI) for the region was performed using geographical information system software (IDRISI, Clark Labs). To exclude impacts from the Minneapolis–St.Paul metropolitan area we restricted the land use and flux data analysis from 15 to 345 degrees from north. Based on the CDL classification, the 2007 land use consisted of ≈32% corn, 11% soybean, 23% grassland, 12% woodland, 10% wetland and 9% developed land within a 5 km radius. Within a 15 km radius the land use consisted of 36% corn, 12% soybean, 22% grassland, 8% woodland, 10% wetland and 9% developed

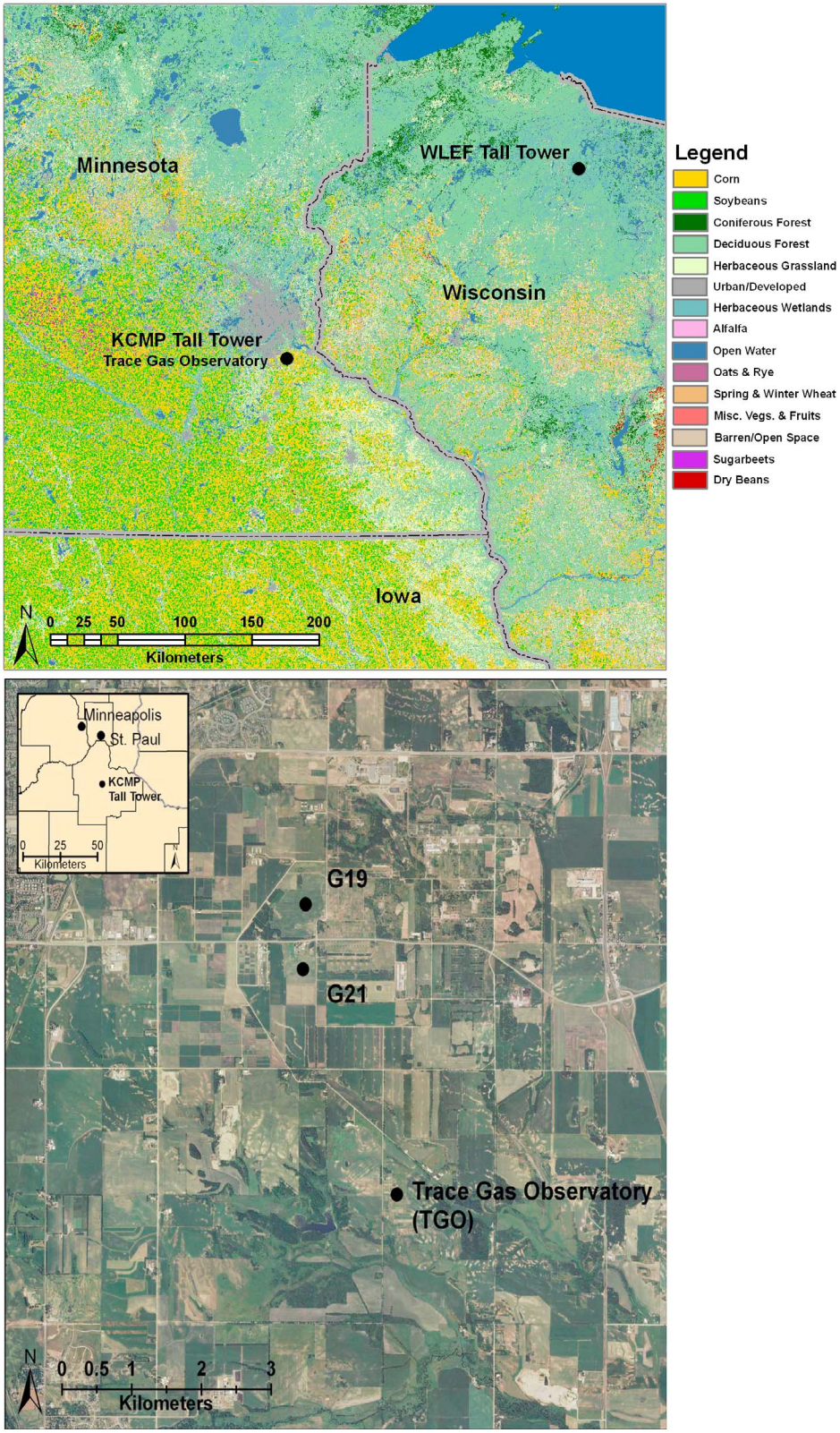

Figure 1. (top) Research site and land use within the vicinity of the tall tower Trace Gas Observatory (TGO) near St. Paul, Minnesota, United States. (bottom) Air photo illustrating the location of TGO in relation to the field-scale AmeriFlux eddy covariance tower sites including G21 and G19 that were used to support the tall tower analyses.

land. Similarity in land use heterogeneity persisted out to approximately 100 km [*USDA-NASS*, 2007a; *Corcoran*, 2009]. The 2008 USDA classification revealed similar patterns, but one noticeable difference was significantly less corn (≈24% contribution) at each scale. Based on the hybrid classification scheme, *Corcoran* [2009] estimated that corn accounted for 41% and 31% of the land use within a 5 km radius of the tall tower in 2007 and 2008, respectively. The land surface heterogeneity is clearly complex, but surprisingly consistent, exhibiting self similarity/scale independence. Flux measurements from the tall tower, should therefore, be representative of the broader region (i.e., 10s of kilometers).

3.3. Carbon Isotope and Micrometeorological Measurements

[20] The carbon isotope molar mixing ratios $^{12}CO_2$ and $^{13}CO_2$ were measured *in situ* using TDL spectroscopy (TGA100A, Campbell Scientific, Incorporated, Logan, Utah, United States) [*Bowling et al.*, 2003; *Griffis et al.*, 2005]. The TDL was maintained within an air conditioned communications building located at the base of the tower. This TDL system was evaluated for making continuous carbon isotope EC flux measurements over a short homogeneous soybean canopy [*Griffis et al.*, 2008]. The air profile system consisted of 4 sample inlets installed at ≈32, 56, 100, and 200 m which were used to compute F_S^i and concentration gradients. The top two levels were instrumented with sonic anemometer-thermometers (CSAT3, Campbell Scientific, Incorporated) for EC flux measurements. The eddy flux for each isotopologue was obtained using 60 min block averaging. In addition, water vapor fluxes were measured using an infrared gas analyzer (IRGA, LI7000, Licor, Incorporated, Lincoln Nebraska, United States). In the analyses presented here we have focused our attention on the 100 m EC data and concentration gradients calculated from the 100 m and 32 m inlets. Flux footprint estimates were derived using the parameterized version of the three-dimensional Lagrangian stochastic model LPDM-B of *Kljun et al.* [2002, 2004]. Here X_{max} is defined as the distance to which the tower measurements are most sensitive. X_{90} is the 90% isopleth, defining the distance from the tower that represents 90% of the source contribution. A detailed discussion of the isotope calibration procedure, data processing, data quality control, EC-TDL precision, and flux footprint analyses are provided in the auxiliary material.

4. Results and Discussion

4.1. Climate and Phenology

[21] The summer of 2007 can be considered a tale of two seasons. Over the duration of the main study period (DOY 152 to DOY 274) the mean air temperature was 20.7°C (33.8°C maximum and −1.7°C minimum). Cumulative precipitation during this period was ≈518 mm. Mean air temperature exceeded the most recent 30 year climate normal (+1.5°C) and precipitation was significantly above normal (140 mm). However, antecedent soil moisture conditions were very dry and June and July 2007 were both warmer and significantly drier than normal (+1.7°C, +1.2°C and −63 mm and −19 mm, respectively). The U.S. Drought Monitor classified much of the region in the moderate drought category. August and September were significantly wetter than normal (+132 mm and +84mm, respectively). Photosynthetically active radiation and relative humidity were both slightly lower during 2007 compared to 2008. In general, Bowen ratio values were slightly higher in 2007 compared to 2008 (0.51 versus 0.48 for the main study period).

[22] Summer 2008 was slightly cooler and significantly drier compared to 2007 measurement period. Mean, minimum, and maximum air temperatures were 19.7°C, 3.2°C and 32.0°C, respectively. Cumulative precipitation for the growing period was 249 mm, approximately 129 mm below normal. Precipitation in each month was below normal. However, according to the U.S. Drought Monitor much of the region was classified as abnormally dry, but no significant drought occurred because of adequate stored soil water prior to the growing season. Cool spring temperatures in 2008 delayed the onset of leaf emergence relative to 2007.

[23] In 2007 field-scale LAI, measured at the G21 AmeriFlux site (corn phase of the rotation) ranged from 0.3 on DOY 164 to 4.0 on DOY 206. The crop canopy had senesced by DOY 260 and was harvested on DOY 284. Estimates of regional NDVI (derived from clear sky Landsat TM images) ranged from about 0.10 in April 2007 to a maximum of 0.49 in August 2007. Values decreased to 0.39 by 16 September 2007. In 2008 LAI at the field scale ranged from 0.1 (0.2) on DOY 169 to 2.3 (3.0) on DOY 220 at the soybean (corn) sites, respectively. The crop canopies had senesced by about DOY 262 and were harvested on DOY 280 (308), respectively. Regional NDVI ranged from about 0.37 in mid-June 2008 to a maximum of 0.54 in early August 2008. Values decreased to 0.40 by 18 September 2008. Regional NDVI values were relatively high into late September and early October despite crop senescence, indicating that nonagricultural lands, such as grasslands/pasture, are an important feature on the landscape.

4.2. Temporal Variability of F_N, λE, CO_2, and δ_a^{13}

[24] Figure 2 shows the hourly values of F_N, λE, CO_2 mixing ratio, and δ_a^{13} measured over the 2007/2008 study period. Close examination of F_N and λE in 2008 indicate that the growing season length was approximately 155 days with detectable photosynthetic activity occurring from about DOY 130 (9 May) to DOY 285 (11 October). Midsummer maximum uptake of CO_2 was approximately 60 μmol m^{-2} s^{-1} and maximum nighttime losses reached 20 μmol m^{-2} s^{-1}. λE values peaked at about 15 mmol m^{-2} s^{-1}. The range of these hourly flux values is characteristic of agricultural crops growing within the footprint of the tall tower (Figure 3). Notice, however, that nonagricultural lands play an important role in the carbon budget as evidenced by the significant uptake of CO_2 during June at TGO compared to the local agricultural sites (Figure 3). The period of detectable photosynthesis for corn and soybean is only about 100 (90) days, so the nonagricultural portions of the landscape lengthen the CO_2 uptake season by approximately 8 weeks. Mean daily F_N indicated similar CO_2 uptake in 2007 compared to 2008 (2.8 vs 3.1 g C m^{-2} d^{-1}).

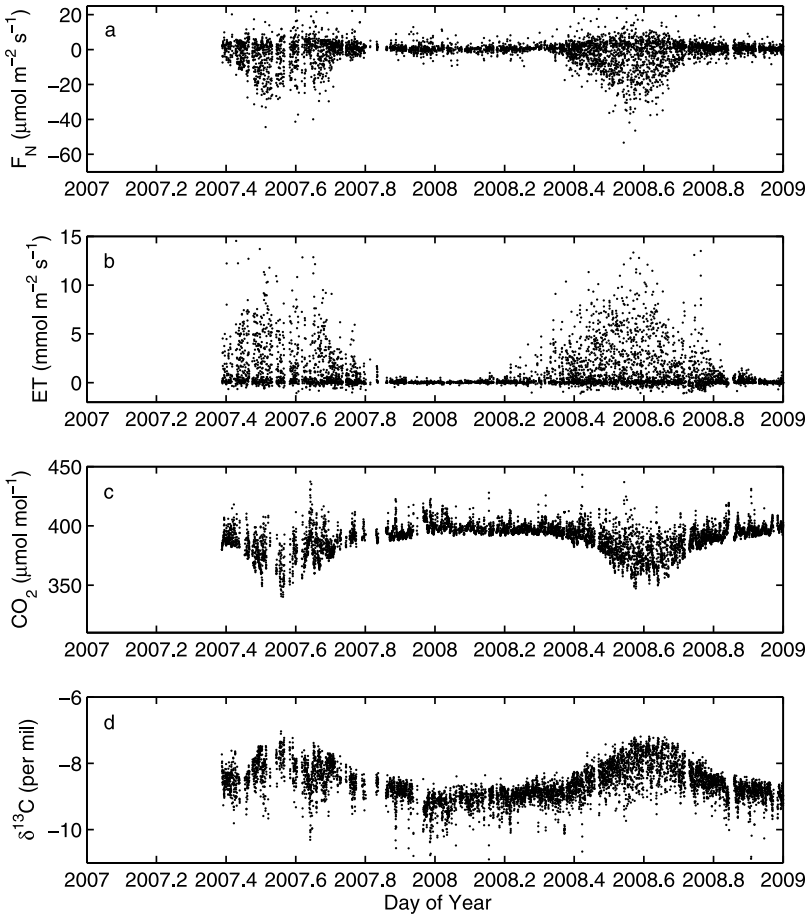

Figure 2. Tall tower time series of (a) net ecosystem CO_2 exchange; (b) evapotranspiration; (c) CO_2 mixing ratio; and (d) carbon isotope composition of CO_2. All values represent hourly averages measured at the 100 m level.

[25] The maximum drawdown in boundary layer CO_2 mixing ratio to about 346 μmol mol^{-1} occurred on DOY 211 approximately 10 days after the observed maximum in the net uptake of CO_2. Growing season δ_a^{13} values reached a maximum of about −7.2‰ on DOY 201 and corresponded closely with F_N. CO_2 mixing ratios reached a maximum of 443 μmol mol^{-1} with δ_a^{13} value of −10.7‰. These values were correlated with northerly flow and associated urban plumes. We applied a harmonic curve fit to the midday (1000 to 1600 LST) CO_2 mixing ratio values (100 m level) in 2008 and determined a seasonal amplitude (one half the peak-to-peak variation) of 9.7 μmol mol^{-1}. The same analysis was applied to δ_a^{13} and yielded an amplitude of 0.39‰. The seasonal amplitude of CO_2 mixing ratio at TGO is in excellent agreement with other tall tower observations from within the upper Midwest, United States [*Miles et al.*, 2009; *Corbin et al.*, 2010].

[26] Analysis of mixing ratio and isotope ratio data from the WLEF tall tower (located in the Chequamegon National Forest (45.9459°N, 90.2723°W, 472 m ASL) in Wisconsin, approximately 260 km to the northeast of the KCMP TGO tall tower(Figure 1)) and the marine boundary layer, at the same latitude, indicate an amplitude of 7.4 μmol mol^{-1} and 4.8 μmol mol^{-1} and 0.39 and 0.30‰, respectively (data source: Globalview-CO_2, 2009, http://www.esrl.noaa.gov/gmd/ccgg/globalview/co2/co2_intro.html). The larger amplitudes observed at TGO can partially be attributed to the lower measurement height (100 m at TGO versus 400 m at WLEF), but are also likely explained by the stronger CO_2 fluxes within this agricultural region [*Miles et al.*, 2009; *Corbin et al.*, 2010].

[27] Diurnal patterns (100 m level) of CO_2 mixing ratio and δ_a^{13} are shown for June, July, August, and September 2008 in Figure 4. These patterns reveal a diurnal amplitude of approximately 8.3, 11.9, 10.4, and 6.3 μmol mol^{-1} for CO_2 and 0.28, 0.38, 0.37, and 0.22‰, for δ_a^{13} for the respective months and indicate that regional-scale CO_2 fluxes and photosynthetic discrimination peaked during July and August. As discussed in more detail below, the diurnal patterns and amplitude of δ_a^{13} can be related directly to the isotopic forcing.

4.2.1. C_4 Flux Footprint Contribution

[28] In general, growing season midday X_{max} and X_{90} were approximately 600 and 1600 m, respectively (Figure 5). Nighttime (stable conditions) values were 750 and 2000 m. Very similar results have been reported for the tall tower

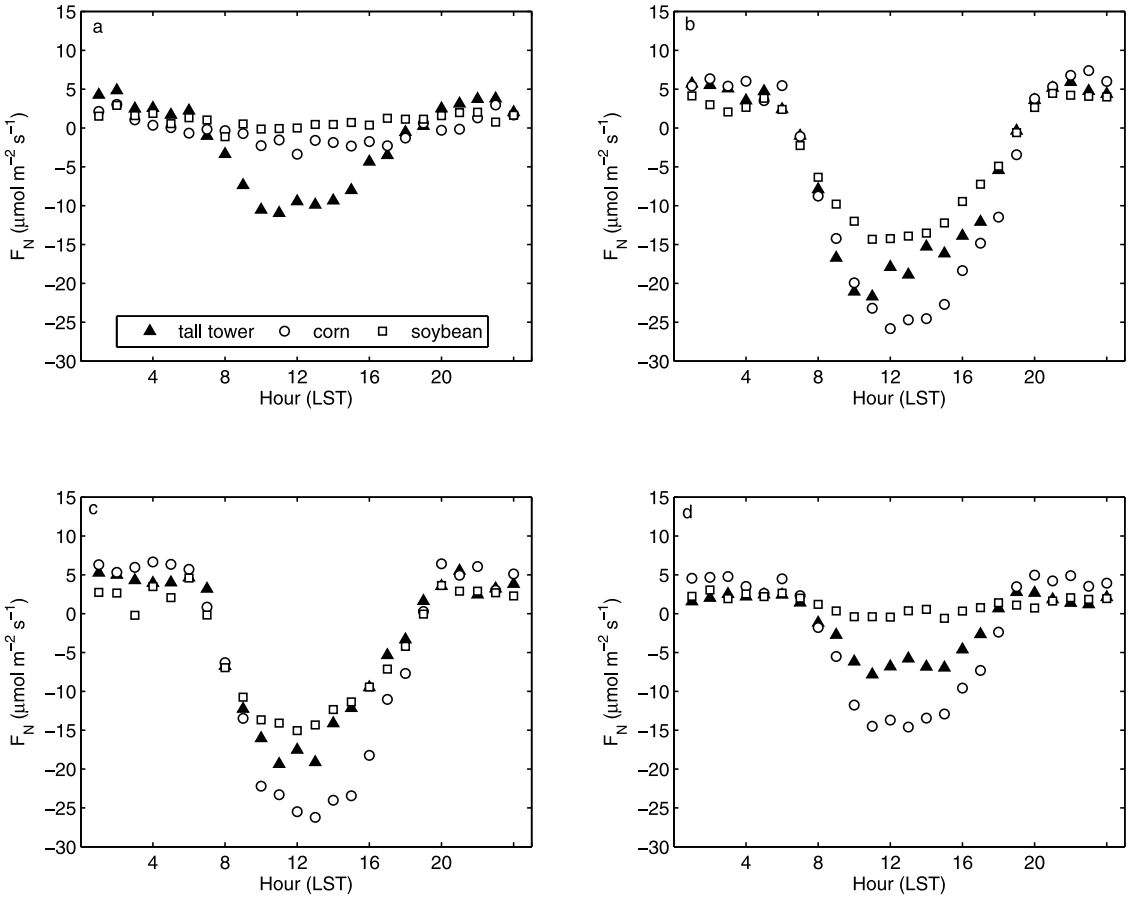

Figure 3. Ensemble diurnal patterns of net ecosystem CO_2 exchange measured during 2008 for (a) June, (b) July, (c) August, and (d) September at the tall tower Trace Gas Observatory and simultaneously at the G19 (corn phase) and G21 (soybean phase) AmeriFlux sites. Approximately 70% of the hourly flux data are presented in each panel (i.e., 30% of the observations are either missing due to instrument failure or were filtered from the analyses based on the quality control criteria).

site in Hungary [*Barcza et al.*, 2009]. Combination of the daytime flux footprint and GIS analyses revealed that 27% of the footprint had a C_4 "origin" during the 2007 and 2008 growing seasons. Surprisingly, the flux footprint analyses between the two growing seasons was less than 1% despite the absolute 10% difference in C_4 land use between the years. This might be an artifact of using a footprint model that does not consider the cross wind contribution or a subtle difference in meteorology between the years (i.e., differences in wind direction or atmospheric stability). Nighttime analyses revealed that 30% of the flux footprint had a C_4 origin. The nighttime stable atmospheric conditions resulted in extended footprints with a slightly stronger C_4 contribution. Therefore, a small land use bias results from differences between daytime and nighttime flux footprints. The differences among June, July, August, and September were insignificant, presumably because of averaging over a relatively long period. Significant differences, however, could be observed for individual days. For example, on DOY 243, 2007 the daytime C_4 contribution was less than 10%.

4.2.2. Flux Ratio Analysis and C_3/C_4 Isotope Partitioning

[29] The isotopic flux ratio analysis, using the EC and flux-gradient methods, is shown in Figure 6 for daytime growing season conditions. Here, the flux ratio analysis was performed with all valid data collected over for the main growing period (June through September or DOY 152 to DOY 274) in order to improve the signal-to-noise ratio and to get a growing season perspective on the relative influence of C_3 versus C_4 vegetation. The data in Figure 6 illustrate excellent agreement between both methods and that the precision of the flux-gradient method is significantly better (<0.2‰) indicating that the EC isotopic flux data have significantly lower signal-to-noise ratio because the fluctuations in the scalars are relatively small at 100 m. Higher precision on the flux-gradient method is a direct result of the very large (70 m) separation distance between inlets. The concentration gradients, therefore, are relatively large, more easily resolved by the TDL, and more reliable for evaluating the differences between months and growing seasons.

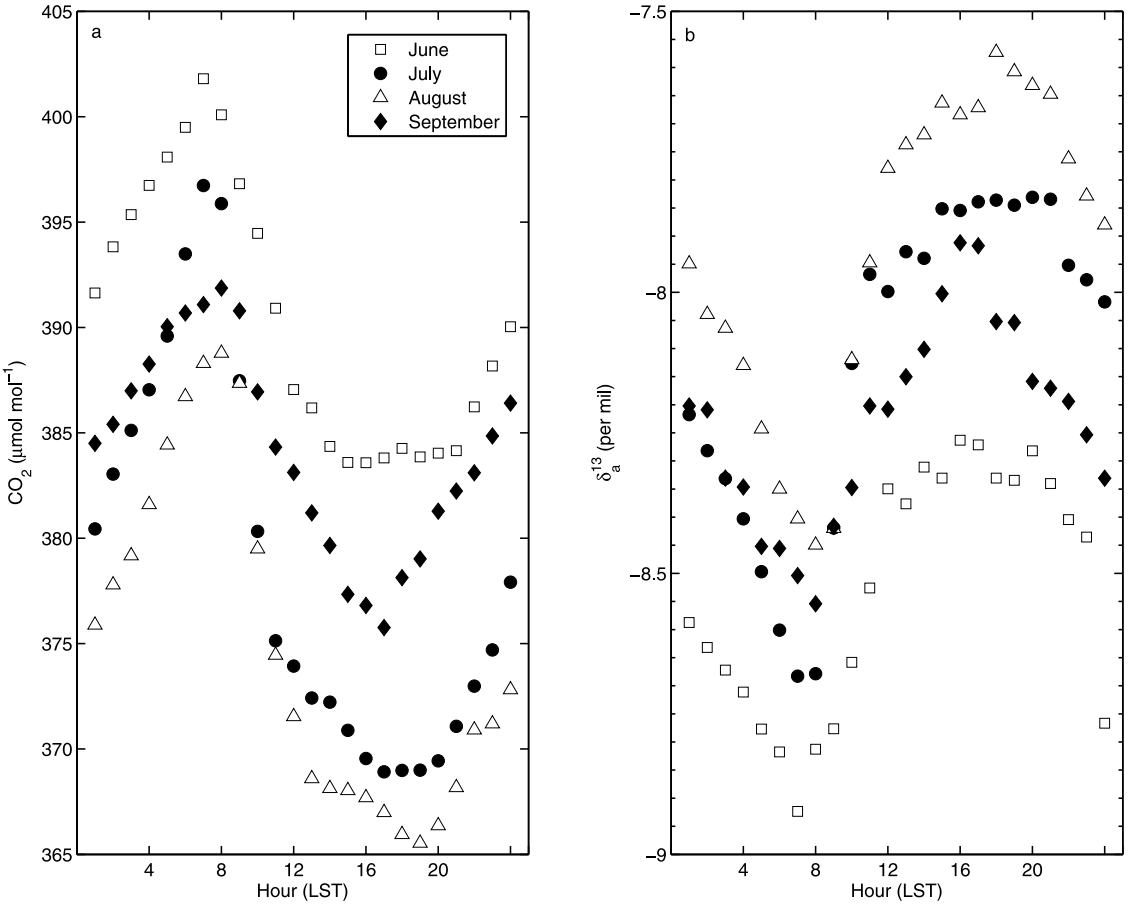

Figure 4. Ensemble diurnal patterns of (a) CO_2 mixing ratio and (b) carbon isotope composition of CO_2. Mean hourly values, measured at the 100 m level of the tall tower Trace Gas Observatory, are shown for June through September 2008. Approximately 75% of the hourly concentration and isotope ratio data are presented in each panel (i.e., 25% of the observations are either missing due to instrument failure or were filtered from the analyses based on the quality control criteria).

[30] We estimated daytime δ_N (isotope composition of F_N) values of −19.3 ± 0.18‰ and −22.5 ± 0.14‰ for 2007 and 2008, respectively (Table 1). Nighttime analyses showed that δ_N (i.e., δ_R) was −20.2 ± 0.06‰ and −22.1 ± 0.06‰ for 2007 and 2008, respectively. Based on the conservation of mass (using equation (6)), with photosynthesis estimated by subtracting nighttime respiration from daytime F_N, we estimated δ_P (Δ, photosynthetic discrimination) values of −19.8 (11.8‰) and −22.3 (14.3‰) for 2007 and 2008. This same flux ratio analysis was performed using monthly phenological windows for June, July, August and September (Table 1). Daytime Δ values were 14.2, 11.5, 12.1, 12.5‰ in 2007 and 14.7, 12.4, 14.8, and 17.4‰ in 2008. In general, the photosynthetic discrimination appears to be stronger in 2008. Both the USDA and hybrid land use classification indicate a C_4 reduction of up to 10% in 2008. Assuming that variation in photosynthetic discrimination is mainly driven by changes in C_4 land use, a back-of-the-envelope calculation indicates that the flux-weighted discrimination would likely increase by about 2 to 3‰, which supports our tall tower flux ratio observations. However, it is also possible that the drought-like conditions of spring and early summer of 2007 lowered photosynthetic discrimination across the region due to an increase in stomatal resistance. In general, C_3 photosynthetic discrimination has been shown to decrease with increasing atmospheric vapor pressure deficit [*Bowling et al.*, 2002] and has been shown to increase with increasing precipitation [*Pataki et al.*, 2003; *Suits et al.*, 2005; *Diefendorf et al.*, 2010]. The challenge of resolving the interannual variability in the isotope composition of F_N and its cause has also been recognized by *Miller et al.* [2003].

[31] Based on a two end member mixing model,

$$f_3 = \frac{\delta_P - \delta_4}{\delta_3 - \delta_4} \tag{12}$$

and using the same end members (for reference) as *Bakwin et al.* [1995], $\delta_3 = -26‰$ and $\delta_4 = -11‰$, we estimated the relative contribution of C_3 vegetation (f_3) to the total F_P for the entire growing period and June, July, August, and September. This analysis assumes that the variation in Δ is driven predominantly by changes in land use. Further, this mixing model yields a partitioning sensitivity of about 7% for a 1‰ change in photosynthetic discrimination. During

Table 1. Photosynthetic $^{13}CO_2$ Discrimination and C_3/C_4 Flux Partitioning

	δ_N (‰)	r^2	n	δ_R (‰)	r^2	n	Δ^a (‰)	f_3
				Year 2007				
June to Sept	−19.3 ± 0.18	0.9999	470	−20.2 ± 0.06	0.9999	685	11.8 ± 0.30	0.59 ± 0.05
June[b]	−19.5 ± 4.2	0.9992	14	−24.6 ± 0.40	0.9999	13	14.2 ± 2.1	0.75 ± 0.15
July[b]	−19.6 ± 0.61	0.9998	168	−19.4 ± 0.21	0.9999	137	11.5 ± 0.43	0.57 ± 0.06
August	−19.7 ± 0.25	0.9999	228	−20.1 ± 0.08	0.9999	296	12.1 ± 0.30	0.61 ± 0.05
September	−20.5 ± 0.62	0.9997	212	−20.5 ± 0.22	0.9999	356	12.5 ± 0.34	0.63 ± 0.05
Median	−19.6 ± 0.61			−20.2 ± 0.21			12.1 ± 0.34	0.61 ± 0.05
				Year 2008				
June to Sept	−22.5 ± 0.14	0.9999	1124	−22.1 ± 0.06	0.9999	1173	14.3 ± 0.38	0.75 ± 0.06
June	−24.9 ± 0.71	0.9994	276	−21.1 ± 0.24	0.9999	264	14.7 ± 0.74	0.78 ± 0.08
July	−20.2 ± 0.54	0.9996	338	−20.7 ± 0.13	0.9999	301	12.4 ± 0.43	0.63 ± 0.06
August	−22.6 ± 0.18	0.9999	284	−23.0 ± 0.10	0.9999	290	14.8 ± 0.29	0.79 ± 0.06
September	−26.0 ± 0.75	0.9995	210	−23.8 ± 0.17	0.9999	305	17.4 ± 0.65	0.96 ± 0.08
Median	−22.6 ± 0.54			−22.1 ± 0.13			14.7 ± 0.43	0.78 ± 0.06

[a]Flux-weighted photosynthetic discrimination (Δ) was calculated from mass balance using measurements of daytime and nighttime net ecosystem CO_2 exchange and the daytime and nighttime discrimination values shown above. All δ_N and δ_R values were derived from geometric type II regression analysis of tall tower isotopic gradients weighted by net ecosystem CO_2 exchange measured using the eddy covariance technique (flux ratio approach). Their uncertainty values represent the standard error of the regression parameter. f_3 represents the relative C_3 gross photosynthetic partitioning. The uncertainty in Δ and f_3 was propagated from the individual measurement contributions and is described in the auxiliary material.

[b]Note these calculations were derived from gradient measurements using the 100 m and 200 m levels. All other calculations were based on gradients derived using the 100 m and 32 m levels on the tall tower.

the mid-to-late growing period (July to August) C_4 plants (corn and some grassland species) had their maximum influence on the carbon budget and the isotopic composition of the atmosphere. Table 1 illustrates that the late growing season CO_2 flux had a strong C_4 composition, suggesting that 40 to 45% of the gross photosynthetic flux had a C_4 origin. Over the entire growing period the C_4 contribution was ≈40% in 2007 and 20% in 2008. Using end members measured directly at our site with $\delta_3 = -26‰$ and $\delta_4 = -12‰$ [*Griffis et al.*, 2007], the f_3 partitioning described above decreased by less than 3%.

[32] At WLEF air samples are collected routinely by ESRL-NOAA in flasks for carbon isotope ratio analyses [*Bakwin et al.*, 1998]. Keeling mixing model analyses indicate that Δ (in this case an approximation based on $\delta_a^{13} - \delta_R$) was about 16.8‰ during the midgrowing season. *Bakwin et al.* [1998] noted that the WLEF isotope signal was strongly influenced by agricultural ecosystems (C_4) in the upper Midwest. The regional-scale estimate of C_4 influence based on the WLEF data indicate a contribution of about 10% at peak growth. At TGO, located about 260 km to the southwest of WLEF, Δ varied by 3 to 5‰ over the growing season and δ_N was 2 to 5‰ more enriched in ^{13}C relative to at WLEF. Based on observations from the North Carolina tall tower site (35.37°N, 77.39°W, May–October 1992–1994), located about 1700 km southeast of TGO, *Bakwin et al.* [1995] estimated a regional C_4 contribution (mainly corn) in the Southeastern United States of ≈23%. Finally, *Miller et al.* [2003] reported a δ_N value of −20.2‰ for a tall tower in Utah (39.90°N, 113.72°W, May–October 1993–2001), indicating a similar C_4 contribution as at the Minnesota TGO site.

[33] *Lai et al.* [2003] also used a micrometeorological/isotope approach to determine the relative importance of C_4 species to F_N in a tall grass prairie (Rannells Flint Hills prairie) near Manhattan, Kansas. Their data showed that C_4 species accounted for ≈68% of the flux during early spring to nearly 100% by late summer. Further, based on a novel boundary layer budget approach, *Lai et al.* [2006] estimated the regional biosphere-atmosphere discrimination near the same site and found that it ranged from about 6 to 1‰ during the growing season, indicating a late-season transition where CO_2 exchange was dominated by C_4 species. *Still et al.* [2003b] investigated the relative contribution of C_4 species to F_N at a grassland pasture site in Oklahoma over a 2 year period. The C_4 contribution increased from ≈38% in spring (April 1999) to nearly 90% in early fall (September 1999). In 2000 the seasonal variation in the relative C_4 flux contribution was significantly less, ranging from 67% in spring (early May) to 77% in midsummer (late July).

[34] The recent modeling study by *Scholze et al.* [2008] accounted for the influence of C_4 crops on the global photosynthetic discrimination averaged over the period 1985 to 1995. Their analyses indicate that inclusion of C_4 crops significantly lowered the global flux-weighted annual Δ value. For a latitudinal band from 15 to 50°N (including the North American Corn Belt), the addition of C_4 cropland lowered Δ by 1.5‰. In the vicinity of the TGO, simulated Δ values ranged from 12 to 16‰ and 16 to 18‰ with and without C_4 crops prescribed. The former range of values are in excellent agreement with our tall tower observations and help substantiate the conclusions of *Scholze et al.* [2008].

[35] *Miller et al.* [2003] provided a broader perspective of $^{13}CO_2$ discrimination based on the NOAA/CMDL Cooperative Air Sampling Network from tall tower sites throughout North America, Europe, and Asia. Their analyses revealed that there was not a significant latitudinal gradient in pho-

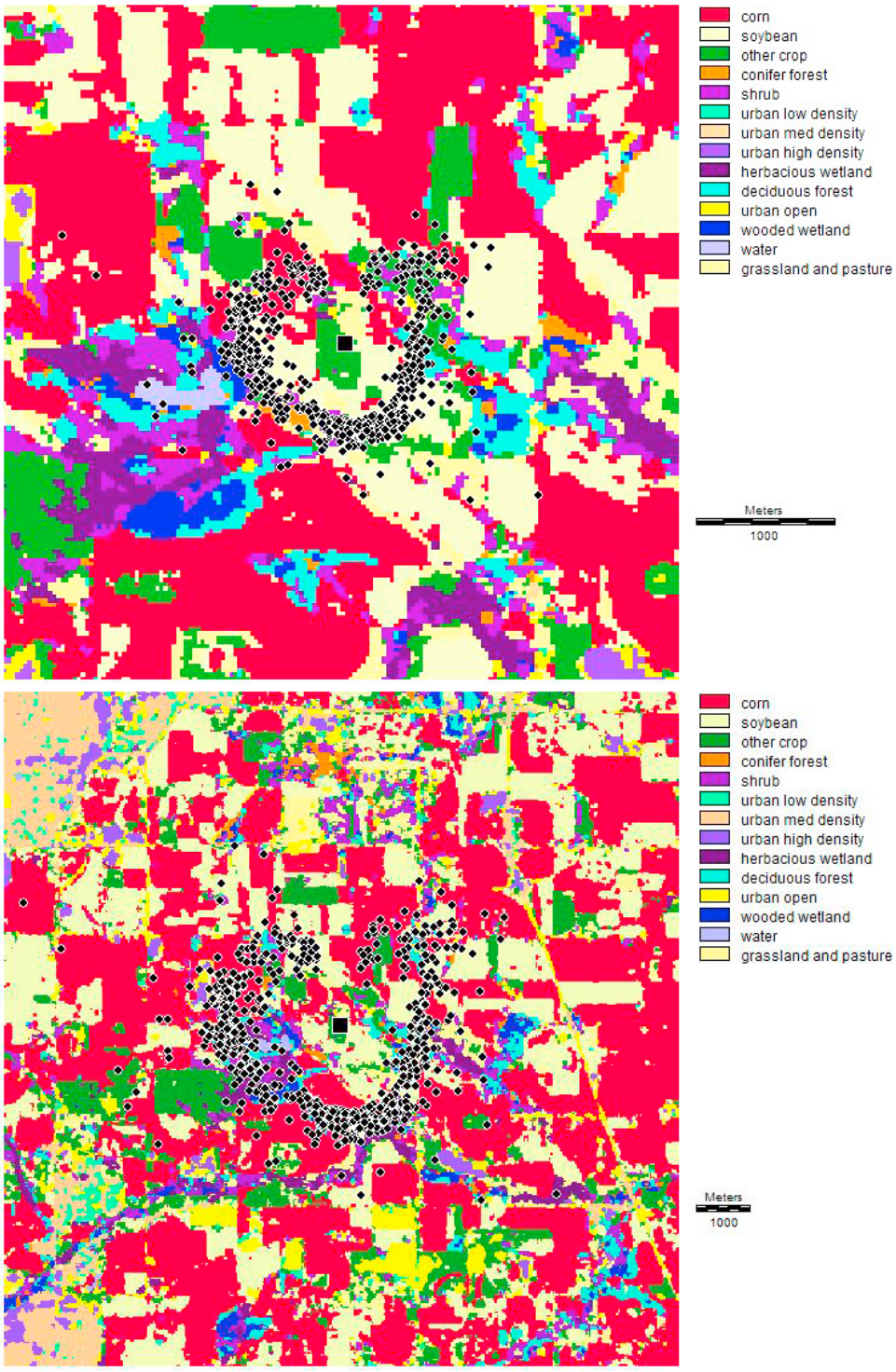

Figure 5. Flux footprint climatology for the tall tower Trace Gas Observatory. Flux footprints were estimated using the parameterized version of the three-dimensional Lagrangian stochastic model LPDM-B. The distance to which the flux is most sensitive (X_{max}) is plotted in the upper panel on a land use map that was derived using a combination of air photos, ground reference data obtained within a 5 km radius of the tall tower, and Landsat TM images at 30 m resolution. The 90% isopleth is plotted in the lower panel. The flux footprint data shown are for the daytime 2007 growing season.

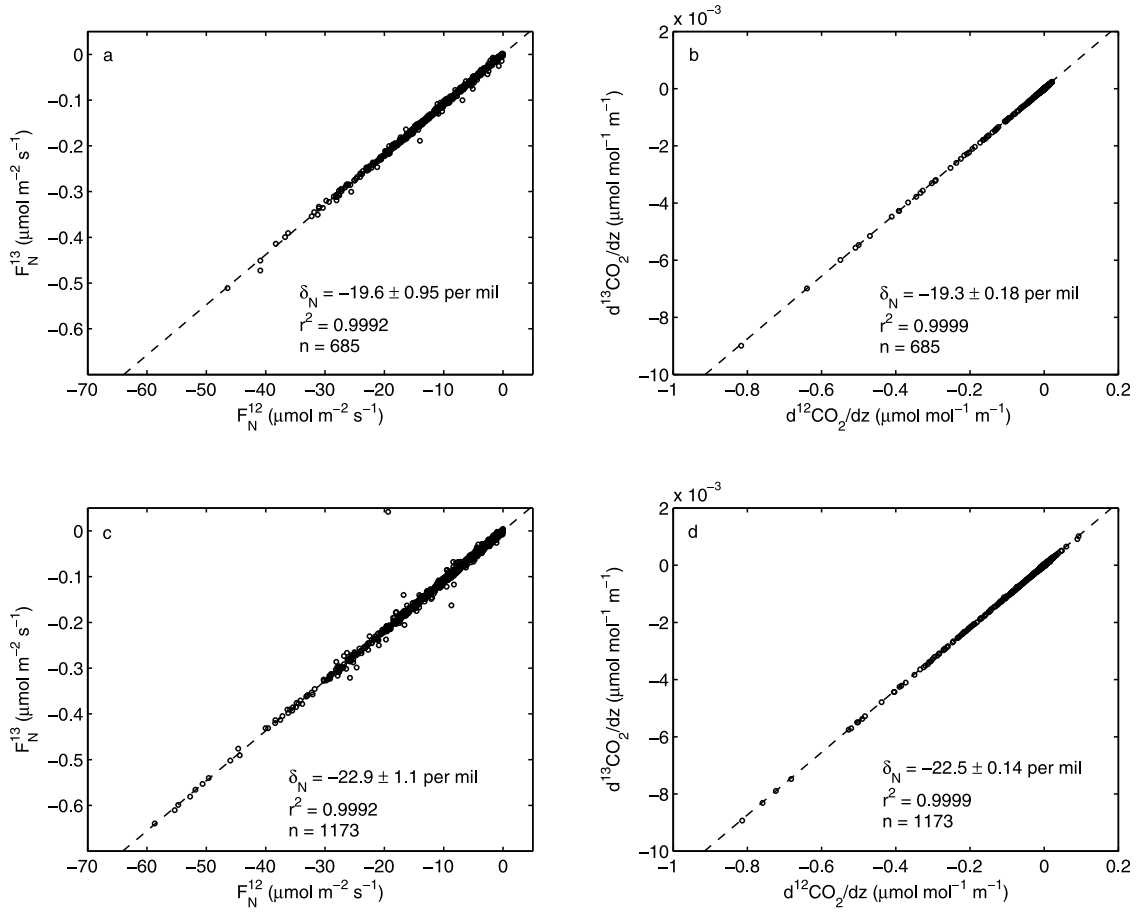

Figure 6. Isotope flux ratio analysis for (a) daytime growing season 2007 based on the eddy covariance approach; (b) daytime growing season 2007 based on the flux-gradient approach; (c) daytime growing season 2008 based on the eddy covariance approach; and (d) daytime growing season 2008 based on the flux-gradient approach. Data points represent hourly isotopic CO_2 eddy covariance flux measurements from the 100 m level at the tall tower Trace Gas Observatory. The gradients (Figures 6b and 6d) were determined as the difference in isotopic mixing ratios between the 100 m and 32 m levels. These gradients were then weighted by the total CO_2 flux for each hour. Dashed lines represent the best fit type II regression analysis.

tosynthetic discrimination as indicated by model simulations [*Fung et al.*, 1997]. However, they concluded that North America had a lower discrimination value compared to Asia and Europe, because of the significant contribution of C_4 vegetation to photosynthesis. We expect that these differences will be exacerbated if C_4 (corn) agricultural production is increased to meet future biofuel demands outlined in the United States Energy Policy Act.

4.2.3. Isotopic Forcing on the Atmosphere

[36] Tall tower EC measurements of the isotopic forcing (I_F) are shown in Figure 7 as ensemble diurnal patterns for June, July, August, and September. The simulated/scaled-up I_F (from equations (6) through (11)) are also presented for the C_3 and C_4 contributions to help verify the above C_3/C_4 partitioning results. The measured I_F from the tall tower indicates that the midday maximum ranged from about 0.012 to 0.018 m/s ‰ in June. The isoforcing observed at the tall tower in June was significantly larger than the scaled-up estimate from the ecosystem-scale data. In fact, given the phenological stage of the C_4 canopy, with daytime respiration slightly exceeding photosynthesis, resulted in a small negative isoforcing over the entire diurnal period. These observations further support the importance of non-agricultural lands contributing to the regional carbon and atmospheric $^{13}CO_2$ budget prior to crop maturity. In order to force better agreement between the June tall tower observations and the simulated values, an increase in the field-scale photosynthetic CO_2 flux by nearly threefold was required.

[37] The amplitude of the observed tall tower isoforcing for June was 0.006 m/s ‰. Assuming a typical planetary boundary layer (PBL) depth ranging from about 200 m to 1500 m over the diurnal period, based on the analysis of *Holzworth* [1964] and using data from the European Center for Medium Range Weather Forecasting, ERA-40, suggests that the amplitude in δ_a^{13} should be about 0.20‰. This

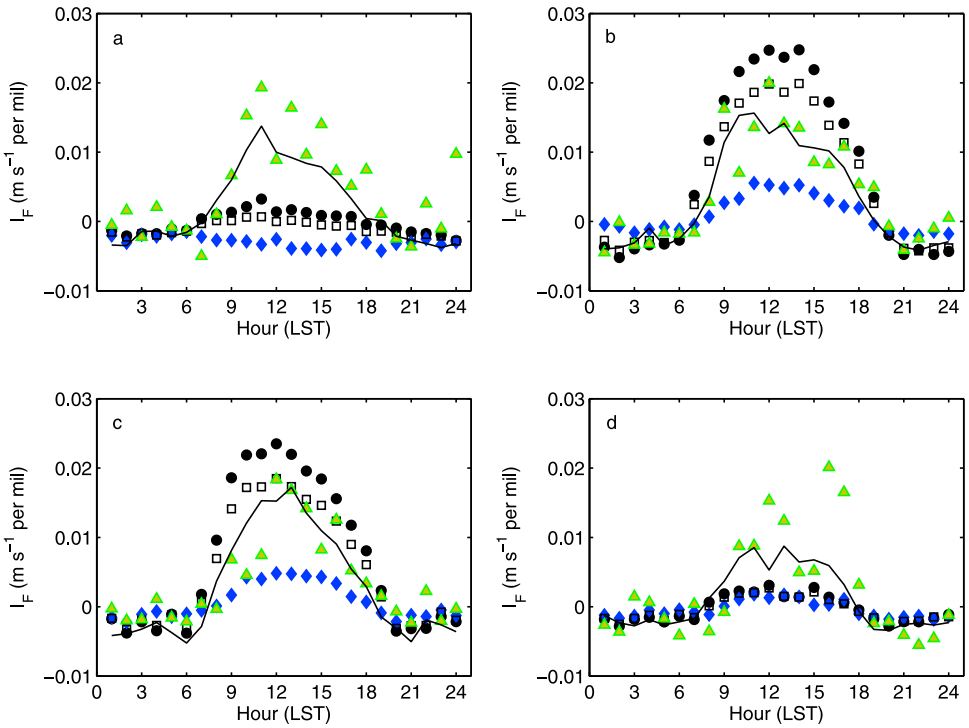

Figure 7. Isotopic forcing analysis for (a) June, (b) July, (c) August, and (d) September 2008. Black circles represent the hourly values of isotopic forcing simulated for a C_3 canopy using field-scale data from the Ameri- Flux site G21. Equations (6) to (11) were used to determine the isoforcing values. A similar analysis is shown for the C_4 (corn) canopy (blue diamonds). These data were obtained from the AmeriFlux site G19. The ecosystem-scale isotopic forcing (squares) represents the scaled-up values of the C_3 and C_4 contributions based on the tall tower flux footprint analysis. The isotopic forcing was also measured directly at the tall tower using the eddy covariance approach (i.e., $\overline{w'\delta'}$, green triangles) and was also calculated (black line) using the monthly flux ratio (gradient) analysis (Table 1) in combination with equation (7).

agrees reasonably well with the observed δ_a^{13} amplitude for June (0.28‰). Although it is a rough estimate, it provides an independent check on the tall tower isoforcing calculation and measurement. The diurnal variation in δ_a^{13} is not only dependent on the surface flux, but is influenced by boundary layer dynamics and rectification [*Chen et al.*, 2006]. *Chen et al.* [2006] showed that the diurnal and seasonal variation of δ_a^{13} due to rectification was ≈0.07 and 0.2‰ above a boreal forest.

[38] Figure 7 also reveals that the observed I_F was greatest during July (0.020 m/s ‰) and August (0.018 m/s ‰). Agreement between tall tower measurements and scaled-up values was relatively good for July and August. Maximum I_F values measured with the EC technique over a soybean canopy within close proximity to the tall tower were typically 0.03 m/s ‰ at midday [*Lee et al.*, 2009]. The amplitude of the tall tower I_F observations at peak growth ranged from 0.007 to 0.009 m/s ‰. Assuming a diurnal range in PBL depth from 200 to 1500 m suggests that the amplitude in δ_a^{13} should be about 0.30‰, which agrees reasonably well with observations (0.37 to 0.38‰ for July and August). The simulated I_F values indicate that the C_4 influence is relatively small primarily because of the small photosynthetic discrimination. While the analysis above shows a strong C_4 influence on the total CO_2 exchange, the relatively small isoforcing illustrates the dominant role of C_3 photosynthetic discrimination on the atmospheric budget of δ_a^{13} and its seasonal and diurnal variability.

[39] A change in land use and its impact on the atmospheric isotopic budget is difficult to assess directly. It requires the use of coupled land surface and atmospheric models that can account for the feedback between the land surface and PBL [*Chen et al.*, 2006; *Barr and Betts*, 1997; *Betts et al.*, 2007]. However, if we consider a simple scenario of increasing corn acreage in the upper Midwest from the current distribution of about 30% to 60% (i.e., trading C_3 crop for C_4 crop as indicated in the United States new Energy Policy Act), we expect that the peak growing season (July/August) midday isoforcing would likely decrease from 0.018 m/s ‰ to 0.012 m/s ‰ (33%) and that the flux-weighted regional discrimination would decrease by about 6‰. The amplitude of the diurnal isoforcing would also decrease by 0.004 m/s ‰ and would cause a decrease in the amplitude of δ_a^{13}. Our analyses suggest the change would be subtle (≈0.13‰), but this would depend on the influence of the changing land surface characteristics and their impact on

PBL depth, entrainment, surface layer humidity, etc. These mechanisms and feedbacks are the subject of ongoing modeling research.

5. Conclusions

[40] Isotopic CO_2 mixing ratios and flux measurements were made from the tall tower Trace Gas Observatory (TGO) located south of St. Paul, Minnesota, in the upper midwestern United States. The data examined here extend from 1 June 2007 to 1 October 2008 and represent the first near-continuous and direct measurements of isotopic CO_2 exchange from a tall tower. In this study we have explored some potential new ways of assessing and tracking the influence of land use change on carbon cycling and their impact on the isotopic composition of the atmosphere. We found that the local and regional land use varied considerably between 2007 and 2008 with significantly more corn (C_4) production in 2007 due to increased demand for biofuel. The 2007 growing season was also strongly influenced by dry antecedent soil moisture conditions and experienced moderate drought over much of the growing period. The isotope composition of net ecosystem CO_2 exchange and photosynthetic $^{13}CO_2$ discrimination was estimated using a combination of eddy covariance and flux-gradient techniques. The photosynthetic discrimination values generally ranged from 11.5 to 14.2‰ in 2007 and 12.4 to 17.4‰ in 2008. These results reveal the potential importance of land use and climate impacts and the effect of C_4 vegetation on $^{13}CO_2$ discrimination. Isotopic partitioning showed that C_4 species accounted for as much as 45% of the gross photosynthetic flux during peak growth in 2007, but generally accounted for about 20 to 40% of the growing season photosynthetic CO_2 exchange. The isoforcing analysis presented here revealed that C_3 discrimination dominated the atmospheric δ_a^{13} budget, especially during spring and fall. A modeling investigation is ongoing to help better understand the impact of land use versus climate variations on photosynthetic discrimination within this heterogeneous landscape.

[41] **Acknowledgments.** We express our sincere thanks to Jeremy Smith and Bill Breiter for their technical assistance in the lab and at the field site. Funding for this research has been provided by the National Science Foundation, ATM-0546476 (T.G.) and by the Office of Science (BER) U.S. Dept. of Energy, DE-FG02-06ER64316 (T.G. and J.B.). We would like to thank Minnesota Public Radio (KCMP 98.3) and Tom Nelson for providing logistical support for this project. The Dietz Brothers climbing crew are recognized for installing, and maintaining our instrumentation on the KCMP tower. We acknowledge the use of the European Center for Medium Range Weather Forecasting, ERA-40 boundary layer height data. We thank four anonymous Reviewers for their detailed assessment of the manuscript. Finally, we gratefully acknowledge the many helpful conversations with Xuhui Lee, Yale University, regarding the tall tower flux measurements and the isotopic forcing principle.

References

Badeck, F.-W., G. Tcherkez, S. Nogués, C. Piel, and J. Ghashghaie (2005), Post-photosynthetic fractionation of stable carbon isotopes between plant organs: A widespread phenomenon, *Rapid Comm. Mass Spectrom.*, *19*, 1381–1391.

Baker, J. M., and T. J. Griffis (2005), Examining strategies to improve the carbon balance of corn/soybean agriculture using eddy covariance and mass balance techniques, *Agric. For. Meteorol.*, *128*, 163–177.

Bakwin, P. S., P. P. Tans, C. L. Zhao, W. Ussler, and E. Quesnell (1995), Measurements of carbon-dioxide on a very tall tower, *Tellus Ser. B*, *47*(5), 535–549.

Bakwin, P. S., P. P. Tans, J. W. C. White, and R. J. Andres (1998), Determination of the isotopic (C-13/C-12) discrimination by terrestrial biology from a global network of observations, *Global Biogeochem. Cycles*, *12*(3), 555–562.

Barcza, Z., A. Kern, L. Haszpra, and N. Kljun (2009), Spatial representativeness of tall tower eddy covariance measurements using remote sensing and footprint analysis, *Agric. For. Meteorol.*, *149*, 795–807.

Barr, A., and A. Betts (1997), Radiosonde boundary layer budgets above a boreal forest, *J. Geophys. Res.*, *102*, 29,205–29,212.

Bathellier, C., F.-W. Badeck, P. Couzi, S. Harscoët, C. Mauve, and J. Ghashghaie (2008), Divergence in $\delta^{13}C$ of dark respired CO_2 and bulk organic matter occurs during the transition between heterotrophy and autotrophy in *Phaseolus vulgaris* plants, *New Phytol.*, *177*, 406–418.

Berger, B. W., K. J. Davis, C. X. Yi, P. S. Bakwin, and C. L. Zhao (2001), Long-term carbon dioxide fluxes from a very tall tower in a northern forest: Flux measurement methodology, *J. Atmos. Oceanic Technol.*, *18*(4), 529–542.

Betts, A. K., R. L. Desjardins, and D. Worth (2007), Impact of agriculture, forest and cloud feedback on the surface energy budget in BOREAS, *Agric. For. Meteorol.*, *142*(2–4), 156–169, doi:10.1016/j.agrformet.2006.08.020.

Bowling, D. R., P. P. Tans, and R. K. Monson (2001), Partitioning net ecosystem carbon exchange with isotopic fluxes of CO_2, *Global Change Biol.*, *7*(2), 127–145.

Bowling, D. R., N. G. McDowell, B. J. Bond, B. Law, and J. R. Ehleringer (2002), ^{13}C content of ecosystem respiration is linked to precipitation and vapor pressure deficit, *Oecologia*, *131*, 113–124.

Bowling, D. R., N. G. McDowell, J. M. Welker, B. J. Bond, B. E. Law, and J. R. Ehleringer (2003), Oxygen isotope content of CO_2 in nocturnal ecosystem respiration: 2. short-term dynamics of foliar and soil component fluxes in an old-growth ponderosa pine forest, *Global Biogeochem. Cycles*, *17*(4), 1124, doi:10.1029/2003GB002082.

Buchmann, N., and J. R. Ehleringer (1998), CO_2 concentration profiles, and carbon and oxygen isotopes in C_3, and C_4 crop canopies, *Agric. For. Meteorol.*, *89*(1), 45–58.

Cerling, T., J. Harris, B. MacFadden, M. Leakey, J. Quade, V. Eisenmann, and J. Ehleringer (1997), Global vegetation change through the Miocene/Pliocene boundary, *Nature*, *389*(6647), 153–158.

Chen, B. Z., J. M. Chen, P. P. Tans, and L. Huang (2006), Simulating dynamics of C13 of CO_2 in the planetary boundary layer over a boreal forest region: covariation between surface fluxes and atmospheric mixing, *Tellus Ser. B*, *58*(5), 537–549.

Ciais, P., et al. (1995), Partitioning of ocean and land uptake of CO_2 as inferred by $\delta^{13}C$ measurements from the NOAA Climate Monitoring and Diagnostics Laboratory Global Air Sampling network, *J. Geophys. Res.*, *100*, 5051–5070.

Corbin, K. D., A. S. Denning, E. Y. Lokupitiya, A. E. Schuh, N. L. Miles, K. J. Davis, S. Richarson, and I. T. Baker (2010), Assessing the impact of crops on regional CO_2 fluxes and atmospheric concentrations, *Tellus Ser. B*, doi:10.1111/j.1600-0889.2010.00485.x, in press.

Corcoran, J. (2009), Assessing the spatial variability of net ecosystem CO_2 production in the upper Midwest, Master's thesis, Univ. of Minn.

Davis, K. J., P. S. Bakwin, C. X. Yi, B. W. Berger, C. L. Zhao, R. M. Teclaw, and J. G. Isebrands (2003), The annual cycles of CO_2 and H_2O exchange over a northern mixed forest as observed from a very tall tower, *Global Change Biol.*, *9*(9), 1278–1293.

Diefendorf, A. F., K. E. Mueller, S. L. Wing, P. L. Koch, and K. H. Freeman (2010), Global patterns in leaf C-13 discrimination and implications for studies of past and future climate, *Proc. Natl. Acad. Sci. U. S. A.*, *107*(13), 5738–5743, doi:10.1073/pnas.0910513107.

Donner, S., and C. Kucharik (2008), Corn-based ethanol production compromises goal of reducing nitrogen export by the Mississippi River, *Proc. Natl. Acad. Sci. U. S. A.*, *105*, 4513–4518.

Drewitt, G. B., C. Wagner-Riddle, and J. S. Warland (2009), Isotopic CO_2 measurements of soil respiration over conventional and no-till plots in fall and spring, *Agric. For. Meteorol.*, *149*, 614–622.

Edwards, E. J., and C. J. Still (2008), Climate, phylogeny and the ecological distribution of C_4 grasses, *Ecol. Lett.*, *11*(3), 266–276, doi:10.1111/j.1461-0248.2007.01144.x.

Ehleringer, J., T. Cerling, and B. Helliker (1997), C_4 photosynthesis, atmospheric CO_2 and climate, *Oecologia*, *112*(3), 285–299.

Farquhar, G. D. (1983), On the nature of carbon isotope discrimination in C_4 species, *Austral. J. Plant Physiol.*, *10*(2), 205–226.

Farquhar, G. D., J. R. Ehleringer, and K. T. Hubick (1989), Carbon isotope discrimination and photosynthesis, *Annu. Rev. Plant Physiol. Plant Molecul. Biol.*, *40*, 503–537.

Finnigan, J. (1999), A comment on the paper by lee (1998), On micrometeorological observations of surface-air exchange over tall vegetation, *Agric. For. Meteorol.*, *97*(1), 55–64.

Flanagan, L. B., and J. R. Ehleringer (1998), Ecosystem-atmosphere CO_2 exchange: interpreting signals of change using stable isotope ratios, *Trends Ecol. Evol.*, *13*(1), 10–14.

Fung, I., et al. (1997), Carbon 13 exchanges between the atmosphere and biosphere, *Global Biogeochem. Cycles*, *11*(4), 507–533.

Ghashghaie, J., M. Duranceau, F. W. Badeck, G. Cornic, M. T. Addeline, and E. Deleens (2001), $\delta^{13}C$ of CO_2 respired in the dark in relation to $\delta^{13}C$ of leaf metabolites: Comparison between *Nicotiana sylvestris* and *Helianthus annuus* under drought, *Plant Cell Environ.*, *24*, 505–515.

Griffis, T. J., J. M. Baker, S. D. Sargent, B. D. Tanner, and J. Zhang (2004), Measuring field-scale isotopic CO_2 fluxes with tunable diode laser absorption spectroscopy and micrometeorological techniques, *Agric. For. Meteorol.*, *124*(1–2), 15–29, 38.

Griffis, T. J., X. Lee, J. M. Baker, S. D. Sargent, and J. Y. King (2005), Feasibility of quantifying ecosystem-atmosphere $C^{18}O^{16}O$ exchange using laser spectroscopy and the flux-gradient method, *Agric. For. Meteorol.*, *135*(1–4), 44–60, 61.

Griffis, T. J., J. Zhang, J. M. Baker, N. Kljun, and K. Billmark (2007), Determining carbon isotope signatures from micrometeorological measurements: Implications for studying biosphere-atmosphere exchange processes, *Boundary Layer Meteorol.*, *123*(2), 295–316.

Griffis, T. J., S. D. Sargent, J. M. Baker, X. Lee, B. D. Tanner, J. Greene, E. Swiatek, and K. Billmark (2008), Direct measurement of biosphere-atmosphere isotopic CO_2 exchange using the eddy covariance technique, *J. Geophys. Res.*, *113*, D08304, doi:10.1029/2007JD009297.

Haszpra, L., Z. Barcza, K. J. Davis, and K. Tarczay (2005), Long-term tall tower carbon dioxide flux monitoring over an area of mixed vegetation, *Agric. For. Meteorol.*, *132*(1–2), 58–77.

He, H., and R. Smith (1999), Stable isotope composition of water vapor in the atmospheric boundary layer above the forests of new england, *J. Geophys. Res.*, *104*, 11,657–11,673.

Holzworth, G. (1964), Estimates of the mean maximum mixing depths in the contiguous united states, *Mon. Weather Rev.*, *92*, 235–242.

Homer, C., et al. (2007), Completion of the 2001 national land cover database for the conterminous united states, *Photogramm. Eng. Remote Sens.*, *73*, 337–341.

Huang, J., X. Lee, and E. G. Patton (2008), A modelling study of flux imbalance and the influence of entrainment in the convective boundary layer, *Boundary Layer Meteorol.*, *127*(2), 273–292, doi:10.1007/s10546-007-9254-x.

Ito, A. (2003), A global-scale simulation of the CO_2 exchange between the atmosphere and the terrestrial biosphere with a mechanistic model including stable carbon isotopes, 1953–1999, *Tellus, Ser. B*, *55*(2), 596–612.

Keeley, J., and P. Rundel (2005), Fire and the Miocene expansion of C_4 grasslands, *Ecol. Lett.*, *8*(7), 683–690, doi:10.1111/j.1461-0248.2005.00767.x.

Keeling, C. D. (1958), The concentration and isotopic abundances of atmospheric carbon dioxide in rural areas, *Geochim. Cosmochim. Acta*, *13*, 322–334.

Kljun, N., M. W. Rotach, and H. P. Schmid (2002), A three-dimensional backward lagrangian footprint model for a wide range of boundary-layer stratifications, *Boundary Layer Meteorol.*, *103*(2), 205–226.

Kljun, N., P. Calanca, M. W. Rotachhi, and H. P. Schmid (2004), A simple parameterisation for flux footprint predictions, *Boundary Layer Meteorol.*, *112*(3), 503–523.

Lai, C. T., A. J. Schauer, C. Owensby, J. M. Ham, and J. R. Ehleringer (2003), Isotopic air sampling in a tallgrass prairie to partition net ecosystem CO_2 exchange, *J. Geophys. Res.*, *108*(D18), 4566, doi:10.1029/2002JD003369.

Lai, C. T., J. R. Ehleringer, P. Tans, S. C. Wofsy, S. P. Urbanski, and D. Y. Hollinger (2004), Estimating photosynthetic C-13 discrimination in terrestrial CO_2 exchange from canopy to regional scales, *Global Biogeochem. Cycles*, *18*, GB1041, doi:10.1029/2003GB002148.

Lai, C. T., A. J. Schauer, C. Owensby, J. M. Ham, B. Helliker, P. P. Tans, and J. R. Ehleringer (2006), Regional CO_2 fluxes inferred from mixing ratio measurements: Estimates from flask air samples in central Kansas, USA, *Tellus, Ser. B*, *58*(5), 523–536.

Lee, X. (1998), Micrometeorological observations of surface-air exchange over tall vegetation, *Agric. For. Meteorol.*, *91*, 39–49.

Lee, X., S. Sargent, R. Smith, and B. Tanner (2005), In-situ measurement of the water vapor $^{18}O/^{16}$ O isotope ratio for atmospheric and ecological applications, *J. Atmos. Oceanic Technol.*, *22*, 555–565.

Lee, X., T. Griffis, J. Baker, K. Billmark, K. Kim, and L. Welp (2009), Canopy-scale kinetic fractionation of atmospheric carbon dioxide and water vapor isotopes, *Global Biogeochem. Cycles*, *23*, GB1002, doi.10.1029/2008GB003331.

Lloyd, J., and G. D. Farquhar (1994), ^{13}C discrimination during CO_2 assimilation by the terrestrial biosphere, *Oecologia*, *99*, 201–215.

Marquis, M., and P. Tans (2008), Carbon crucible, *Science*, *320*, 460–461.

Marschner, F. (1974), The original vegetation of Minnesota (redraft of the original 1930 edition), technical report, N. Centr. For. Exp. Sta., For. Serv., U.S. Dept. of Agric., St. Paul, Minn.

McDowell, N., et al. (2008), Understanding the stable isotope composition of biosphere-atmosphere CO_2 exchange, *EOS Trans. AGU*, *89*(10), 94–95, doi:10.1029/2008EO100002.

Miles, N., et al. (2009), Atmospheric results from the nacp's mid continent intensive field campaign, in 8*th International Carbon Dioxide Conference* (*ICDC*8), Jena, Germany.

Miller, J. B., P. P. Tans, J. W. C. White, T. J. Conway, and B. W. Vaughn (2003), The atmospheric signal of terrestrial carbon isotopic discrimination and its implication for partitioning carbon fluxes, *Tellus, Ser. B*, *55*, 197–206.

Monfreda, C., N. Ramankutty, and J. A. Foley (2008), Farming the planet: 2. Geographic distribution of crop areas, yields, physiological types, and net primary production in the year 2000, *Global Biogeochem. Cycles*, *22*, GB1022, doi:10.1029/2007GB002947.

Osborne, C., and D. Beerling (2006), Nature's green revolution: The remarkable evolutionary rise of C-4 plants, *Philos. Trans. R. Soc. B*, *361*(1465), 173–194, doi:10.1098/rstb.2005.1737.

Pataki, D. E., J. R. Ehleringer, L. B. Flanagan, D. Yakir, D. R. Bowling, C. J. Still, N. Buchmann, J. O. Kaplan, and J. A. Berry (2003), The application and interpretation of keeling plots in terrestrial carbon cycle research, *Global Biogeochem. Cycles*, *17*(1), 1022, doi:10.1029/2001GB001850.

Rayner, P., I. Enting, R. Francey, and R. Langenfelds (1999), Reconstructing the recent carbon cycle from atmospheric CO2, delta C-13 and O-2/N-2 observations, *Tellus, Ser. B*, *51*(2), 213–232.

Rayner, P. J., R. M. Law, C. E. Allison, R. J. Francey, C. M. Trudinger, and C. Pickett-Heaps (2008), Interannual variability of the global carbon cycle (1992–2005) inferred by inversion of atmospheric CO2 and delta (CO2)-C-13 measurements, *Global Biogeochem. Cycles*, *22*, GB3008, doi:10.1029/2007GB003068.

Riley, W. J., C. J. Still, M. S. Torn, and J. A. Berry (2002), A mechanistic model of (H2O)-O-18 and (COO)-O-18 fluxes between ecosystems and the atmosphere: Model description and sensitivity analyses, *Global Biogeochem. Cycles*, *16*(4), 1095, doi:10.1029/2002GB001878.

Sage, R. (2001), Environmental and evolutionary preconditions for the origin and diversification of the C-4 photosynthetic syndrome, *Plant Biol.*, *3*(3), 202–213.

Scholze, M., P. Ciais, and M. Heimann (2008), Modeling terrestrial ^{13}C cycling: Climate, land use and fire, *Global Biogeochem. Cycles*, *22*, GB1009, doi:10.1029/2006GB002899.

Smith, B. (1989), Origins of agriculture in eastern north america, *Science*, *246*, 1566–1571.

Still, C. J., J. A. Berry, G. J. Collatz, and R. S. DeFries (2003a), Global distribution of C-3 and C-4 vegetation: Carbon cycle implications, *Global Biogeochem. Cycles*, *17*(1), 1006, doi:10.1029/2001GB001807.

Still, C. J., J. A. Berry, M. Ribas-Carbo, and B. R. Helliker (2003b), The contribution of C-3 and C-4 plants to the carbon cycle of a tallgrass prairie: An isotopic approach 3, *Oecologia*, *136*(3), 347–359.

Suits, N. S., A. S. Denning, J. A. Berry, C. J. Still, J. Kaduk, J. B. Miller, and I. T. Baker (2005), Simulation of carbon isotope discrimination of the terrestrial biosphere, *Global Biogeochem. Cycles*, *19*, GB1017, doi:10.1029/2003GB002141.

Tans, P. P. (1980), On calculating the transfer of carbon-13 in reservoir models of the carbon cycle, *Tellus, Ser. B*, *32*, 464–469.

Tcherkez, G., S. Nogués, J. Bleton, G. Cornic, F. W. Badeck, and J. Ghashghaie (2003), Metabolic origin of carbon isotope composition of leaf dark-respired CO_2 in French bean, *Plant Physiol.*, *131*, 237–244.

USDA-NASS (2007a), Cropland data layer, prepared by the Natl. Agric. Stat. Serv., U. S. Dept. of Agric., Washington, D. C.

USDA-NASS (2007b), Agricultural statistics database, prepared by the Natl. Agric. Stat. Serv., U. S. Dept. of Agric., Washington, D. C.

Wittenberg, U., and G. Esser (1997), Evaluation of the isotopic disequilibrium in the terrestrial biosphere by a global carbon isotope model, *Tellus Ser. B*, *49*(3), 263–269.

Wyngaard, J., and R. Brost (1984), Top-down and bottom-up diffusion of a scalar in the convective boundary-layer, *J. Atmos. Sci.*, *41*(1), 102–112.

Yakir, D. (2003), The stable isotopic composition of atmospheric CO_2, in *The Atmosphere, Treatise on Geochemistry*, edited by H. D. Holland and K. K. Turekian, vol. 4, chap. 4.07, pp. 175–212, Elsevier, Oxford, U. K.

Yakir, D., and L. D. L. Sternberg (2000), The use of stable isotopes to study ecosystem gas exchange, *Oecologia*, *123*(3), 297–311.

Yi, C., K. J. Davis, P. S. Bakwin, B. W. Berger, and L. C. Marr (2000), Influence of advection on measurements of the net ecosystem-atmosphere exchange of CO_2 from a very tall tower, *J. Geophys. Res.*, *105*(D8), 9991–9999.

Zhang, J., T. J. Griffis, and J. M. Baker (2006), Using continuous stable isotope measurements to partition net ecosystem CO_2 exchange, *Plant Cell Environ.*, *29*(4), 483–496.

J. M. Baker, K. Billmark, M. Chen, J. Corcoran, M. Erickson, and T. J. Griffis, Department of Soil, Water, and Climate, University of Minnesota, Saint Paul, MN 55108, USA. (tgriffis@umn.edu)

S. D. Sargent, Campbell Scientific Incorporated, Logan, UT, USA.